Construction of a Metabolic Model for the Human Pathogen *Candida parapsilosis* and Early Identification of Putative Novel Anti-Fungal Drug Targets

Diogo Alexandre Carracedo Couceiro [1,2]

[1] Department of Bioengineering, Instituto Superior Técnico, Universidade de Lisboa, 1049-001 Lisbon, Portugal

[2] Institute for Bioengineering and Biosciences, Biological Sciences Research Group, Instituto Superior Técnico, 1049-001 Lisbon, Portugal

October 2021

1. Abstract

Candida parapsilosis has seen one of the most significant rises in incidence among pathogenic *Candida* spp., often taking second place only to *C. albicans*. Adding to this increased incidence is the rise in resistance to first line antifungals and lack of adequate alternative therapeutics, not only for *C. parapsilosis* but throughout the genus. Genome Scale Metabolic Models (GSMMs) have risen as a powerful *in silico* tool for the understanding of pathogenesis due to their systems view of metabolism and, above all, drug target predictive capacity. In this project a metabolic model for the human pathogen *C. parapsilosis* was constructed – *Cpar*MM – comprising 1112 genes, 598 proteins, 2892 reactions and 2885 metabolites across four compartments. Upon extensive manual curation this model was experimentally validated and proven to quantitatively predict biomass production, as well as predict *C. parapsilosis'* ability to use several metabolites as sole carbon or nitrogen sources. From the resulting validated model, a list of predicted essential genes common to other major pathogenic *Candida* spp. in mimicked host conditions was obtained. Among these predicted drug targets, 18 were found to be entirely new, for which no previous inhibitor was ever assigned. Additionally, Fol1, Abz1, Cab1 and Cab5 seem to be rather promising putative novel drug targets, as they represent the possibility of inducing systemic metabolic impairment by targeting central metabolism.

Key Words: *C. parapsilosis*; Genome Scale Metabolic Model; Resistance; Antifungals; Fungaemia.

2. Introduction

In a world of climatic and consequent social change, human susceptibility to microbial disease is increased. In particular, fungal infections have seen a significant rise in incidence worldwide since the 1980's, with *Candida* spp. accounting for the majority of cases [1]. Furthermore, although *Candida albicans* is generally still the most common isolate, the 1990s saw a shift in incidence within the genus, towards Non-*Candida albicans Candida* species (NCAC) [2]. From these, *Candida parapsilosis* has seen one of the most significant increases, often surging as the second most common etiological agent of *Candida* spp. infections worldwide, subverting historical trends in species incidence and even outranking

C. albicans in some European countries [3]. Non-geographically restricted and with a broad range of virulence factors, adding to *C. parapsilosis'* already complex pathogenicity, is both the rise in resistance to first-line antifungals and intrinsically lower susceptibility to alternative therapies – such as azoles [4] and echinocandins [1] respectively. Thus, there is a strong need to not only develop new antifungal therapies but also develop new, adequately paced, research tools for the understanding of the metabolism of pathogenesis, how to impair it, impair the pathogen's growth and ultimately impede its consequent establishment of infection.

Genome Scale Metabolic Models (GSMMs) have surged as a Systems Biology approach and solution for this issue [5]. GSMMs correspond to the *in silico* reconstructed metabolic network of a given organism [6] and thus allow for a systems perspective of metabolism. In the little more than 20 years since the publication of the first model [7], GSMMs have proven their applicability and versatility guiding strain design in metabolic engineering, to elucidating novel drug target discovery in molecular medicine[8]. Their applicability stems from their ability to predict the effects of specific reaction disruptions on reactions somewhere else in the network, before any kind of wet-lab setup [9]. As the name itself conveys, GSMMs have as a fundamental principle the idea that the genome, albeit indirectly, codes for the metabolic network of the cell. Thus, the fundamental triad of GSMMs consists of Gene-Protein-Reaction associations (GPR), whose establishment can be done based on the accumulated knowledge of more than a century of biochemical research [9]. Consequently, GSMMs are a platform for the integration of many kinds of information at many different levels and are thus permanently targetable for further complementation and improvement, proving a powerful tool for the future of the metabolic understanding of disease.

In this project a GSMM for the human pathogen *C. parapsilosis* was constructed and validated. From the validated model a set of predicted essential genes and reactions common to other pathogenic *Candida* spp. was obtained, and their targetability as putative novel anti-fungal drug targets was discussed and evaluated.

3. Materials and Methods

The herein described metabolic model reports to the yeast *Candida parapsilosis* with the taxonomic ID 5480. Henceforth, this model will be referred to as *Cpar*MM (*C. parapsilosis* Metabolic Model). Construction was performed using *merlin* 4.0.5 [10] as the basilar software. Model construction comprised two main stages – metabolic network reconstruction and subsequent validation – figure 1. Metabolic network reconstruction comprised an initial semi-automatic obtaining of a draft reconstruction followed by extensive manual curation. Manual curation assured the network's connectivity – this is, assured all biomass precursors' synthesis - and comprised both a pre and a post-compartmentalisation stage. Compartmentalisation was implemented on an already connected and superficially validated network so to simplify compartment related issue solving.

Finally, the model's reaction and gene essentiality were predicted and assessed in mimicked host conditions, and coalesced with predictions from other published models for two other major pathogenic yeasts - *C. albicans*[11] and *C. glabrata* [12].

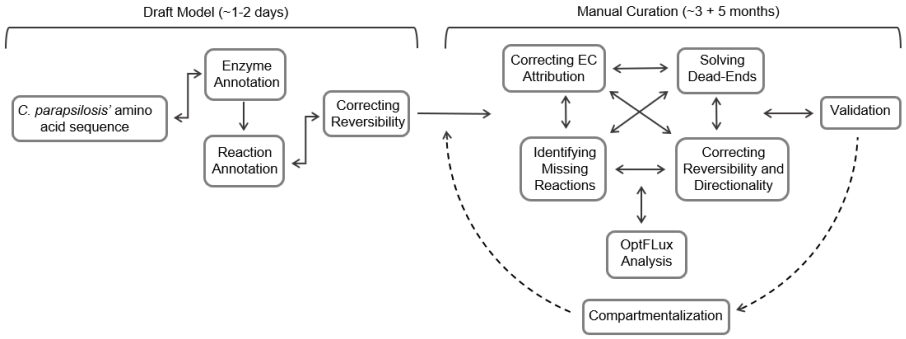

Figure 1: Schematic representation of the general procedure behind the construction of the herein described model. Draft model construction implements mainly automated tools and thus its relatively shorter time span. Manual curation involves a series of non-hierarchical aspects to be assessed and corrected, thus the bidirectional arrows. The workflow of this second stage of curation is similar for both the non- and compartmentalised model.

3.1 Enzyme and Reaction Annotation

Initial draft model construction comprised enzyme and subsequent reaction annotation. Enzyme annotation resulted from the implementation of the Basic Local Alignment Search Tool (BLAST) [13] of *C. parapsilosis'* amino acid sequences against remote databases - UniProt-SwissProt and UniProt-TrEMBL [14]. The amino acid sequences were retrieved from NCBI [15]. Hit selection was based on phylogenetic proximity as described in Tsui *et. al* 2008 [16]. Subsequent reaction annotation resulted from the integration of data from the Kyoto Encyclopedia of Genes and Genomes (KEGG) [17] in the model. Manual curation likewise resorted to the same databases along with literature research.

3.2 Correcting Reaction Reversibility, Directionality and Balance

Initial meta curation was performed with resort to a *merlin* integrated tool which implements information from the remote tool eQuilibrator [18]. Further curation was entirely manual and justified with resort to information from MetaCyc [19] and existing literature. Unbalanced reactions were identified automatically and balancing was performed manually and justified with resort to MetaCyc, CheBi [20], Brenda [21] and existing literature.

2.3 Assuring Network Connectivity

The biomass equation served as the first line criterium in the pipeline of blocked or missing reaction identification. Components of the equation whose production was not assured by the initial draft model – gaps - were first identified individually. Each of these was located in the network, blocked or missing reactions were identified and located, and possible issues assigned. Corrections and reaction addition were justified with resource to literature search, remote databases such as MetaCyc, Brenda, Candida Genome Database (CGD) [22] and UniProt, and to the already validated and published models for *S. cerevisiae* iMM904 [23] and iND750 [24] – all edited reactions are shown in the supplementary excel file S1.

3.4 Compartmentalisation

Compartmentalisation was implemented with resort to WoLF PSORT [25], a protein localization predictor. Compartmentalization was also only implemented on the already connected non-compartmentalised model in order to simplify respective issue solving.

3.5 Biomass Equation

The herein used biomass equation includes data from *C. parapsilosis, Candida albicans, Candida tropicalis* and *Saccharomyces cerevisiae* due to lack of *C. parapsilosis*' specific literature regarding biomass composition. The discerned components of the biomass equation along with their relative content are shown in the supplementary excel file S1.

3.6 Validation

3.6.1 Growth Media and Strains

C. parapsilosis type strain ATCC 22019 was batch cultured at 30 ºC in orbital agitation (250 rpm) in Yeast Extract-Peptone-Dextrose (YPD) for inoculate cultivation, Synthetic Minimal Media (SMM) for growth parameter determination, and Yeast Nitrogen Base either without amino acids or ammonium sulphate for carbon and nitrogen source usage assessment. Media composition are as follows: YPD: 20 g/L glucose (Merck), 20 g/L (Merck) and 10 g/L yeast extract (Merck); SMM: 20g/L (Merck), 2.7 g/L ammonium sulphate, 0.05 g/L magnesium sulphate, 2 g/L potassium dihydrogen phosphate, 0.5 g/L calcium chloride and 100 µg/L biotin; Carbon source assessment with YNB: 5 g/L carbon source and 6.8 g/L YNB without amino acids; Nitrogen source assessment YNB: 5 g/L glucose (Merck), 2.7 g/L nitrogen source and 1.7 g/L YNB without ammonium sulphate. Solid media contained an additional 2 g/L agar (Iberagar).

3.6.3 Assessing Carbon and Nitrogen Source Usage

The model's ability to predict biomass production using several compounds as sole carbon or nitrogen sources was compared to literature based *in vivo* observations. For the few disparate literature based and predicted results wet-lab growth was assessed using the lab isolate *C. parapsilosis* type strain ATCC 22019. Growth was assessed in solid YNB media. Inoculates were first diluted in sterile water to an OD_{600nm} of 0.05. Three consecutive *C. parapsilosis* cell suspensions – 10^{-1}, 10^{-2} and 10^{-3} – were plated as 4 µL spots and the plates were incubated at 30 ºC for 24 hours.

3.6.4 Determining Glucose Consumption Rate in Batch Culture

Cultures for determining the glucose consumption rate ($Y_{x/s}$.mmol.gDCW^{-1}.h^{-1}) were performed in SMM. Inoculates were diluted to an initial OD_{600nm} of 0.3 and incubated at 30 ºC in orbital agitation (250 rpm) for 10 hours. Growth in liquid media was monitored by measuring culture OD_{600nm}. Samples of 4 mL for determining dry biomass and glucose concentration were taken every 2 hours and centrifuged at 13000 rpm for 3 min. The culture supernatant was collected for glucose concentration determination and the pellet was used for determining dry cell weight. Biomass was measured as the mass difference of each sample tube while empty *vs*. after lyophilization of each sample. Glucose concentration was determined by HPLC on an Aminex HPX-87 H Ion Exchange chromatography column eluted with 0.0005 M H_2SO_4 at a flow rate of 0.6 mL/min at room temperature. Concentrations were determined with resource to the adequate calibration curves.

3.7 Simulations and Flux Based Analysis

Simulations were performed using OptFlux [26] and served the assessment of the model's Consumption *vs.* Production profile as well as essentiality predictions – allowing for the tracing of flux through the network. Essentiality predictions were performed in simulated RPMI 1640 medium [27]. Assessment of *Cpar*MM's Consumption *vs.* Production profile was performed in simulated SMM and guided by those of the published models

iND750 for *Saccharomyces cerevisiae* [24] and iRV781 for *C. albicans* [11]. Carbon and nitrogen source assessment were performed in simulated SMM, either substituting the reference glucose or ammonia with the test sources.

4. Results and Discussion

4.1 Model Characteristics

The herein describe metabolic model for *C. parapsilosis* - *Cpar*MM - is a compartmentalised model comprising 1112 genes, 598 proteins, 2892 reactions and 2885 metabolites across four compartments – extracellular, cytoplasm, mitochondria, and peroxisome. Manual curation assessed a total of 408 reactions from which 83 were mass balanced, 162 were corrected in regard to reversibility or directionality, and 163 had their annotation corrected or completed, were added or removed.

CparMM is capable of predicting biomass production at a biologically justifiable nutritional cost coherent with that observed for other published models for *S. cerevisiae* [24] and *C. albicans* [11] – figure 2. Note that biotin consumption by both *Candida* models, while not being present in iND750, results from *Candida* spp. being auxotrophic for this vitamin [28]. Note as well that the production of the chimeric metabolites Pyridoxal phosphate Residue and L-Histidine Residue results from the mass balancing solution implemented on the reaction with the KEGG ID R10686. Furthermore, glycolaldehyde production is also of notice, resulting from its non-connectivity to the network and the impossibility of metabolite accumulation due to the assumption of steady state.

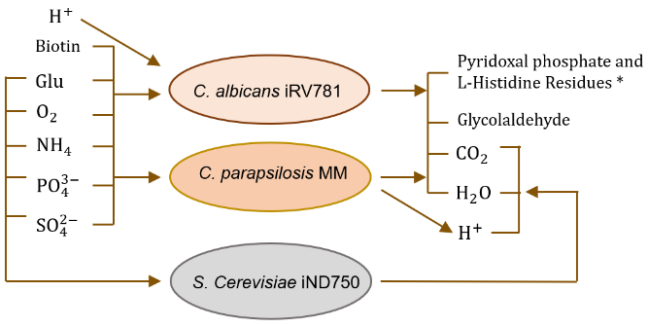

Figure 2: Schematic representation of the consumption/production profiles of the three models, showing their respective similarities and differences. Note both *Candida* spp. models are producing Pyridoxal phosphate and L-Histidine residues, due to the mass balancing solution implemented for the reaction with the KEGG ID R10686. Biotin consumption by both *Candida* models result from *Candida* spp. being biotin auxotrophic.

*Cpar*MM also shows a reliable ability to predict biomass production using different compounds as sole carbon or nitrogen sources, having made 85% correct predictions from the 34 tested compounds – table 1. Furthermore, *Cpar*MM has been shown to make reliable quantitative predictions of rate of biomass production relative to a given corresponding glucose consumption rate. For an experimentally determined glucose consumption rate of 2.098 +/- 0.404 mmol.gDCW^{-1}.h^{-1} *Cpar*MM predicts a specific growth rate of 0.180 h^{-1} being the corresponding experimentally determined 0.159 +/- 0.027 h^{-1}.

Moreover, in simulated RPMI growth medium a total of 129 genes and reactions were predicted as essential in *Cpar*MM, 37 of which were common to the two other foremost pathogenic *Candida* spp. models – *C. albicans* [11] and *C. glabrata* [12].

4.2 Assessing the Predictive Reliability of Carbon and Nitrogen Source Usage

Beyond its Consumption *vs.* Production profile, *Cpar*MM's predictive reliability was further cemented by assessing its ability to predict biomass production using different sole carbon or nitrogen sources relative to *in vivo* observations. In total 34 different carbon and nitrogen sources simulated in SMM were assessed – simulation results shown in table 1. Experimental validation was performed for some initially contradictory results - literature based *vs.* predicted results – by assessing growth in solid media. The results are shown in figure 3 below.

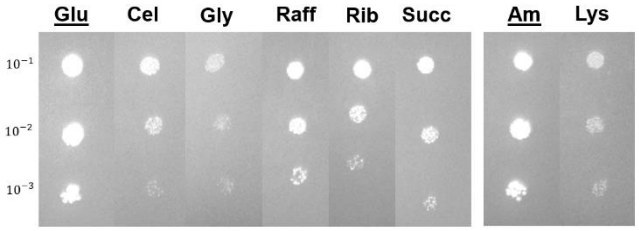

Figure 3: Growth essays on solid YNB medium, 24h incubation at 30ºC, with different sole carbon or nitrogen sources for the experimental validation of contradictory predicted *vs*. literature observed biomass production. **Glu** – glucose (underlined carbon control); **Cel** – cellobiose; **Gly** – glycerol; **Raff** – raffinose; **Rib** – ribose; **Succ** – succinate; **Am** – ammonia (underlined nitrogen control); **Lys** – L- lysine.

Table 1: Simulation results for several different carbon and nitrogen sources alongside in vitro described data. From the 34 different tested compounds, CparMM correctly predicted growth on 85 %. Biomass production is represented by a plus (+), no biomass production by a minus (-) and prediction disparities are in underlined italic. Experimentally validated sources are noted with an asterisk (*).

Carbon Source	Growth		References	Carbon Source	Growth		References	Nitrogen Source	Growth		References
	in silico	*In vivo*			*in silico*	*In vivo*			*in silico*	*In vivo*	
Glucose*	+	+	[29]	**Ethanol**	+	+	[30]	**Ammonia***	+	+	[30]
Maltose	+	+		**Methanol**	-	-		**Nitrite**	-	-	
Sucrose	+	+		**Acetic Acid**	+	+		**Nitrate**	-	-	
Lactose	-	-		**Succinate***	+	+	#	**L-Lysine***	+	+	#
Galactose	+	+		**Inulin**	-	-	[30]	***Ethylamine***	-	+	[30]
Raffinose*	-	+	#	**Ribitol**	-	-		**Creatine**	-	-	
Cellobiose*	+	+		**Ribose***	+	+	#	**D-Tryptophan**	-	-	
Galactitol	-	-	[31]	***Mannitol***	-	+	[30]	***Glucosamine***	+	-	
Trehalose	-	-		**L-Arabinose**	-	-		***Cadaverine***	-	+	
Xylose	+	+		**Citrate**	+	+					
Inositol	-	-		**Erythritol**	-	-					
Salicin	-	-	[30]	**Glycerol***	+	+	#				
Arbutin	-	-									

Although in different extents *C. parapsilosis* is capable of growth in all the tested conditions – figure 3. This results in a *de facto* incorrect prediction for raffinose for which *Cpar*MM predicts no biomass. The case for glycerol as a carbon source not generating biomass might be made, given the significant lesser extent of growth relative to the other plate growths. It could be that growth resulted from residual nutrients from the initial inoculate medium. However, if this was the case the most likely observation would be that while the first dilution (10^{-1}) would result in faint growth, no growth would be observed for any subsequent dilutions – which was not the case. Two possible reasons might explain this observation – *C. parapsilosis* is relatively less efficient in using glycerol as a carbon source and/or initial inoculate optical density was erroneously lesser.

From the 34 tested sources, *Cpar*MM predicts disparate results for five which translates to around 85% correct predictions relative to the 71% prior to curation - and consequently 15% incorrect predictions. Even so, this reflects the reliable predictive capacity of *Cpar*MM. Note the relative extent of manual curation within the greater universe of the model's close to 3000 reactions.

4.3 *Cpar*MM's Growth Parameters: Glucose Consumption Rate *vs.* Specific Growth Rate

Due to lack of literature data regarding *C. parapsilosis'* specific glucose consumption rate and its respective and resulting growth rate in SMM, these parameters were experimentally determined. The main objective of this step was the assessment of how similar the predicted and experimentally determined growth rates were for a corresponding and likewise experimentally determined glucose consumption rate. These parameters were obtained as the slopes of two linear regressions as described in Sauer *et al.* [32]. The experimentally determined parameters along with the corresponding *Cpar*MM predicted specific growth rate value are shown below in table 2.

Table 2: For the experimentally determined glucose consumption rate of 2.098 +/- 0.404 mmol.gDCW^{-1}.h^{-1} *Cpar*MM predicts a specific growth rate of 0.180, relative to the experimentally determined rate of 0.159 +/- 0.027 h^{-1}. The predicted growth rate is within the uncertainty interval of the experimentally determined parameter and thus there is no significant difference between both, reflecting *Cpar*MM's predicate reliability.

	Experimental	**Predicted**
$Y_{X/S}$/ mmol.gDCW^{-1}.h^{-1}	2.098 +/- 0.404	
μ/h^{-1}	0.159 +/- 0.027	0.180

As shown above, for a glucose consumption rate of 2.098 +/- 0.404 mmol.gDCW^{-1}.h^{-1} *Cpar*MM predicts a specific growth rate of 0.180 h^{-1} relative to the experimentally determined 0.159 +/- 0.027 h^{-1}. This predicted value not only is fairly similar to its experimental counterpart, as it is well within its corresponding uncertainty interval which translates in no significant difference between both. This is, *Cpar*MM is curated to an extent that beyond the qualitative verisimilitude discussed previously, it seems to be strikingly reliable also from a quantitative predictive perspective.

4.4 Predicting and Discussing Gene and Reaction Essentiality

A *Cpar*MM simulation in RPMI 1640 medium resulted in a total of 129 predicted putative targets, from which 87 correspond to essential genes and 42 to essential reactions annotated with multiple genes - each of the predicted essential genes or reactions representing putative novel anti-fungal drug targets. As discussed previously, although *C. albicans* is still generally the most frequent cause of infection, other species such as *C. parapsilosis* and *C. glabrata* have seen relevant rises in incidence. Furthermore, in some instances infection is of mixed nature, leading to cases of breakthrough candidemia by species other than *C. albicans* [33]. It is then of interest to try and identify putative targets that span these species in order to maximise their applicability in the long term. Thus, *Cpar*MM's predicted essentiality was intersected with that of other published models for *C. albicans* [11] and *C. glabrata* in the same environmental condition. This intersection resulted in a total of 37 common essential ECs, from which 18 are not associated to any active drug according to the information retrieved from the DrugBank [34] – representing entirely novel putative drug targets. Interestingly, these interception's results also include essential ECs that have already been validated as essential and have associated in-use drugs – such as those annotated to *ERG11* and the *FKS* genes -, conferring an added level of validation to *Cpar*MM's predictive reliability

A first set of foremost interesting genes are the *FOL1* and *ABZ1* genes. Fungi and consequently *Candida* spp. rely on folate *de novo* biosynthesis given their inability to uptake folate from the environment [35]. Targeting these kinds of metabolic chokeholds and thinking from an auxotrophy inducing perspective represents a straightforward way of compromising the cell's growth. Both *FOL1* and *ABZ1* encode proteins responsible for two folate precursor synthesising reactions. Furthermore, these genes do not present human orthologs since human metabolism does not synthesise folate, relying on diet derived folate [35]. Note that the absence of a human ortholog although not an excluding factor, is a preferable attribute since this translates into lower chances of host drug toxicity and may allow for greater freedom of drug design. The dihydropteroate synthase encoded by *FOL1* has been shown to be successfully inhibited by antifolates such as sulfones in a series of microorganisms – from *Escherichia coli* to *Plasmodium falciparum* [34,35]. However, antifolate therapy for *Candida* infections is not particularly effective considering current antifolate compounds [36]. In fact, for *C. albicans* only sulfanilamide is used clinically, although restricted to topical use [37]. Given the efficacy of antifolates in treating infections by other etiologic agents, this might present the opportunity to design new effective antifungal compounds. In its turn the para-aminobenzoate synthetase encoded by *ABZ*1 does not seem to have any assigned drug neither for *Candida* nor for other organisms, and in that sense represents a fully novel putative drug target. On one hand, this putative target might present an alternative to *FOL1* in the possibility of no effective Fol1p targeting compounds. On the other, this might also present the possibility of a combined targeting strategy, referring back to the idea that multiple and simultaneous targeting, although in smaller extents, might be relatively more effective. This is, it could be that this combined therapy could overcome the current inefficacy of antifolate compounds for treating *Candida* spp. infections.

A second set of interesting predicted essential genes common to the three considered species' models are *CAB5* and *CAB1*. Coenzyme A (CoA) is a major if not the major cosubstrate of many biosynthetic reactions across the cell's metabolism - acting as an acyl group carrier for, among others, fatty acid biosynthesis which have a major role in cellular structural integrity. Inhibiting CoA and subsequent Acyl-CoA biosynthesis represents a good manner of inducing general metabolic impairment. Both Cab1p and Cab5p are essential for CoA biosynthesis and thus both these putative targets represent the fundamental possibility of inducing systemic metabolic impairment by targeting one specific metabolite's synthesis. Furthermore, they have already been described as targetable even if to different extents. In this sense they represent a pair of quite relevant and interesting predicted targets.

Furthermore, other predicted essential genes likewise present as interesting putative novel drug targets. A set comprising *URA3, URA4, URA5 and URA7*, and another comprising *ERG7*, *ERG26* and *ERG27*. Justifying these genes' interest are their relative position in the network since each are annotated to consecutive reactions – with the exception of *ERG7*. This consecutiveness presents the possibility of putative alternative combined therapies utilizing inhibiting compounds that although not particularly effective on their own, would cumulatively inhibit these pathway branches for instance. Moreover, the set comprising the *ERG* genes' interest is further cemented by their pertaining to an already targetable pathway – referring back to *ERG11*. Furthermore, the majority of these genes' encoded proteins have been shown to be essential in *C.* albicans and have assigned effective inhibiting compounds in other organisms.

Conclusions and Perspectives

In this project a metabolic model for the human pathogen *C. parapsilosis* was constructed – *Cpar*MM – comprising 1112 genes, 598 proteins, 2892 reactions and 2885 metabolites across four compartments. Upon extensive manual curation this model was experimentally validated and proven to quantitatively predict biomass production, as well as predict *C. parapsilosis'* ability to use several metabolites as sole carbon or nitrogen sources. Still, the model would benefit from a final evaluation step of a number of unconnected reactions which, although not affecting the model's performance when evaluating central metabolism, deserve further scrutiny.

From the resulting validated model a list of predicted essential genes common to other major pathogenic *Candida* spp. in mimicked host conditions was obtained. Among these predicted drug targets 18 were found to be entirely new, for which no previous inhibitor was ever assigned. Additionally, Fol1, Abz1, Cab1 and Cab5 seem to be rather promising putative novel drug targets as they represent the possibility of inducing systemic metabolic impairment by targeting central metabolism. It would be interesting to apply *in silico* docking methodologies to these predicted drug targets, allowing for the selection and designing of inhibitory molecules to be tested as putative novel anti-fungal drugs.

Bibliography

1. Silva, S. *et al.* Candida glabrata, Candida parapsilosis and Candida tropicalis: Biology, epidemiology, pathogenicity and antifungal resistance. *FEMS Microbiol. Rev.* **36**, 288–305 (2012).

2. Fridkin, S. K. The changing face of fungal infections in health care settings. *Clin. Infect. Dis.* **41**, 1455–1460 (2005).

3. Trofa, D., Gácser, A. & Nosanchuk, J. D. Candida parapsilosis, an emerging fungal pathogen. *Clin. Microbiol. Rev.* **21**, 606–625 (2008).

4. Castanheira, M., Deshpande, L. M., Messer, S. A., Rhomberg, P. R. & Pfaller, M. A. Analysis of global antifungal surveillance results reveals predominance of Erg11 Y132F alteration among azole-resistant Candida parapsilosis and Candida tropicalis and country-specific isolate dissemination. *Int. J. Antimicrob. Agents* **55**, 105799 (2020).

5. Gu, C., Kim, G. B., Kim, W. J., Kim, H. U. & Lee, S. Y. Current status and applications of genome-scale metabolic models. *Genome Biol.* **20**, 1–18 (2019).

6. Zhang, C. & Hua, Q. Applications of genome-scale metabolic models in biotechnology and systems medicine. *Front. Physiol.* **6**, 1–8 (2016).

7. Edwards, J. S. & Palsson, B. O. Systems properties of the Haemophilus influenzae Rd metabolic genotype. *J. Biol. Chem.* **274**, 17410–17416 (1999).

8. Kim, T. Y., Kim, H. U. & Lee, S. Y. Metabolite-centric approaches for the discovery of antibacterials using genome-scale metabolic networks. *Metab. Eng.* **12**, 105–111 (2010).

9. Raškevičius, V. *et al.* Genome scale metabolic models as tools for drug design and personalized medicine. *PLoS One* **13**, 1–14 (2018).

10. Dias, O., Rocha, M., Ferreira, C. & Rocha, I. Reconstructing genome-scale metabolic models with merlin. **43**, 3899–3910 (2015).

11. Viana, R. *et al.* Genome-scale metabolic model of the human pathogen candida albicans: A promising platform for drug target prediction. *J. Fungi* **6**, 1–19 (2020).

12. Xu, N. *et al.* Reconstruction and analysis of the genome-scale metabolic network of Candida glabrata. *Mol. Biosyst.* **9**, 205–216 (2013).

13. Altschul, S. F., Gish, W., Miller, W., Myers, E. W. & Lipman, D. J. Basic local alignment search tool. *J. Mol. Biol.* **215**, 403–410 (1990).

14. Bateman, A. UniProt: A worldwide hub of protein knowledge. *Nucleic Acids Res.* **47**, D506–D515 (2019).

15. https://www.ncbi.nlm.nih.gov/Taxonomy/Browser/wwwtax.cgi?mode=Info&id=5480.

16. Tsui, C. K. M., Daniel, H. M., Robert, V. & Meyer, W. Re-examining the phylogeny of clinically relevant Candida species and allied genera based on multigene analyses. *FEMS Yeast Res.* **8**, 651–659 (2008).

17. Kanehisa, M. & Goto, S. KEGG: Kyoto Encyclopedia of Genes and Genomes. *Nucl. Acid Res.* **28**, 27–30 (2000).

18. Flamholz, A., Noor, E., Bar-Even, A. & Milo, R. EQuilibrator - The biochemical thermodynamics calculator. *Nucleic Acids Res.* **40**, 770–775 (2012).

19. Caspi, R. *et al.* The MetaCyc database of metabolic pathways and enzymes and the BioCyc collection of Pathway/Genome Databases. *Nucleic Acids Res.* **42**, 459–471 (2014).

20. Degtyarenko, K. *et al.* ChEBI: A database and ontology for chemical entities of biological interest. *Nucleic Acids Res.* **36**, 344–350 (2008).

21. Schomburg, I., Chang, A. & Schomburg, D. BRENDA, enzyme data and metabolic information. *Nucleic Acids Res.* **30**, 47–49 (2002).

22. Skrzypek, M. S., Binkley, J. & Sherlock, G. Using the candida genome database. *Methods Mol. Biol.* **1757**, 31–47 (2018).

23. Zomorrodi, A. R. & Maranas, C. D. Improving the iMM904 S. cerevisiae metabolic model using essentiality and synthetic lethality data. *BMC Syst. Biol.* **4**, 178 (2010).

24. Duarte, N. C., Herrgård, M. J. & Palsson, B. Reconstruction and validation of Saccharomyces cerevisiae iND750, a fully compartmentalized genome-scale metabolic model. *Genome Res.* **14**, 1298–1309 (2004).

25. Horton, P. *et al.* WoLF PSORT : protein localization predictor. **35**, 585–587 (2007).

26. Rocha, I. *et al.* OptFlux: An open-source software platform for in silico metabolic engineering. *BMC Syst. Biol.* **4**, (2010).

27. Moore, G. E., Gerner, R. E. & Franklin, H. A. Culture of Normal Human Leukocytes. *JAMA J. Am. Med. Assoc.* **199**, 519–524 (1967).

28. Sprenger, M. *et al.* Fungal biotin homeostasis is essential for immune evasion after macrophage phagocytosis and virulence. *Cell. Microbiol.* **22**, 1–19 (2020).

29. Devadas, S. M. *et al.* Auxanographic carbohydrate assimilation method for large scale yeast identification. *J. Clin. Diagnostic Res.* **11**, DC01–DC03 (2017).

30. https://wi.knaw.nl/page/fungal_table.

31. Deorukhkar & Roushani, S. Identification of Candida species: conventional methods in the era of molecular diagnosis. *Ann. Microbiol. Immunol.* **1**, 1002 (2018).

32. Sauer, U. *et al.* Metabolic flux ratio analysis of genetic and environmental modulations of Escherichia coli central carbon metabolism. *J. Bacteriol.* **181**, 6679–6688 (1999).

33. Cuervo, G. *et al.* Breakthrough candidaemia in the era of broad-spectrum antifungal therapies. *Clin. Microbiol. Infect.* **22**, 181–188 (2016).

34. Wishart, D. S. *et al.* DrugBank 5.0: A major update to the DrugBank database for 2018. *Nucleic Acids Res.* **46**, D1074–D1082 (2018).

35. Lawrence, M. C. *et al.* The three-dimensional structure of the bifunctional 6-hydroxymethyl-7,8- dihydropterin pyrophosphokinase/dihydropteroate synthase of Saccharomyces cerevisiae. *J. Mol. Biol.* **348**, 655–670 (2005).

36. Navarro-Martínez, M. D., Cabezas-Herrera, J. & Rodríguez-López, J. N. Antifolates as antimycotics?. Connection between the folic acid cycle and the ergosterol biosynthesis pathway in Candida albicans. *Int. J. Antimicrob. Agents* **28**, 560–567 (2006).

37. Eldesouky, H. E., Mayhoub, A., Hazbun, T. R. & Seleema, M. N. Reversal of azole resistance in Candida albicans by sulfa antibacterial drugs. *Antimicrob. Agents Chemother.* **62**, 1–12 (2018).